The Clinical Respiratory Journal

WILEY

ORIGINAL ARTICLE

TFAP2A Activates S100A2 to Mediate Glutamine Metabolism and Promote Lung Adenocarcinoma Metastasis

Tao Zeng | Wangsheng Ren | Hang Zeng | Dachun Wang | Xianyu Wu | Guo Xu

Department of Cardiothoracic Surgery, Sichuan Mianyang 404 Hospital, Mianyang City, Sichuan Province, China

Correspondence: Guo Xu (xuguoguo2024@163.com)

Received: 15 March 2024 | **Revised:** 3 July 2024 | **Accepted:** 29 July 2024

Funding: The authors received no specific funding for this work.

Keywords: glutamine metabolism | lung adenocarcinoma | metastasis | S100A2 | TFAP2A

ABSTRACT

Background: Lung adenocarcinoma (LUAD) is a fatal disease with metabolic abnormalities. The dysregulation of S100 calcium-binding protein A2 (S100A2), a member of the S100 protein family, is connected to the development of various cancers. The impact of S100A2 on the LUAD occurrence and metastasis, however, has not yet been reported. The functional mechanism of S100A2 on LUAD cell metastasis was examined in this article.

Methods: The expression of TFAP2A and S100A2 in LUAD tissues and cells was analyzed by bioinformatics and qRT-PCR, respectively. The enrichment pathway analysis was performed on S100A2. Bioinformatics analysis determined the binding relationship between TFAP2A and S100A2, and their interaction was validated through dual-luciferase and chromatin immunoprecipitation experiments. Cell viability was determined using cell counting kit-8 (CCK-8). A transwell assay was performed to analyze the invasion and migration of cells. Immunofluorescence was conducted to obtain vimentin and E-cadherin expression, and a western blot was used to detect the expression of MMP-2, MMP-9, GLS, and GLUD1. The kits measured the NADPH/NADP ratio, glutathione (GSH)/glutathione disulfide (GSSG) levels, and the contents of glutamine, α-KG, and glutamate.

Results: S100A2 was upregulated in LUAD tissues and cells, and S100A2 mediated glutamine metabolism to induce LUAD metastasis. Additionally, the transcriptional regulator TFAP2A was discovered upstream of S100A2, and TFAP2A expression was upregulated in LUAD, which indicated that TFAP2A promoted the S100A2 expression. The rescue experiment found that upregulation of S100A2 could reverse the inhibitory effects of silencing TFAP2A on glutamine metabolism and cell metastasis.

Conclusion: In conclusion, by regulating glutamine metabolism, the TFAP2A/S100A2 axis facilitated LUAD metastasis. This suggested that targeting S100A2 could be beneficial for LUAD treatment.

1 | Introduction

One of the most prevalent and deadly cancers, lung cancer, is the primary cause of cancer-related mortality [1]. Furthermore, lung adenocarcinoma (LUAD), which makes up about 40% of all lung cancer cases, is the most prevalent pathological kind of disease [2]. It is usually found at a late stage due to the absence of early diagnostic criteria. Currently, available treatments for LUAD primarily consist of radiotherapy, chemotherapy, molecular targeted therapy, and surgery. However, the survival rate of patients remains extremely low because of the high metastasis rate of LUAD and resistance to chemotherapy and radiotherapy [3, 4]. Therefore, investigating the regulatory mechanism of LUAD development may lead to novel approaches for LUAD patient diagnosis and treatment.

The S100 protein family can regulate different cellular reactions by acting as an intracellular Ca^{2+} sensor. Based on some research, the S100 protein family is connected to the occurrence and progression of many tumor types [5]. S100

© 2024 The Author(s). The *Clinical Respiratory Journal* published by John Wiley & Sons Ltd.

protein is crucial in regulating cell differentiation, proliferation, migration, and other biological functions by interacting with various signaling proteins such as P53 and nuclear factor kappa B (NF-κB), thereby participating in tumor occurrence and development [6, 7]. Pulmonary fibrosis (PF) is a common outcome of various interstitial lung diseases, and Huang et al. demonstrated that low S100A2 expression inhibits the Wnt/β-catenin signaling pathway by inhibiting the transduction of the Wnt/β-catenin signaling pathway and thereby inhibiting the process of epithelial–mesenchymal transition in PF [8]. S100A2, a protein belonging to the S100 family, is essential in several cancers [9]. Previous studies have shown that S100A2 is highly expressed in NSCLC, and its high mRNA expression level can lead to low survival in NSCLC patients [7]. In HCC, upregulated expression of S100A2 resulted in low patient survival, and low expression of S100A2 significantly inhibited the proliferation and migration of HepG2 cells [10]. However, the S100A2 impact on different tumors is inconsistent. Research has revealed that endometrial cancer (EC) tissue exhibits significantly higher levels of S100A2 mRNA and protein compared to normal tissue, and this is associated with a poor survival rate [11]. Han et al. [12] evidenced that in colorectal cancer (CRC), the tumor-associated transcription factor NFYA can be delivered by the S100A2/KPNA2 cotransport complex. NFYA is transported to the nucleus and inhibits the transcriptional activity of E-cadherin, thereby promoting CRC metastasis. In a study of breast cancer (BC), however, S100A2 expression was found to be greatly downregulated in BC tissues and cell lines, and overexpression of miR-325-3p may enhance BC cell invasion and proliferation by downregulating S100A2 expression [13]. Although S100A2 exhibits various physiological and pathological effects in tumors, the mechanism of S100A2 in LUAD cell metastasis is still unclear. Thus, further exploration into the function mechanism of S100A2 in the LUAD occurrence and metastasis is necessary to develop new therapies. Glutamine is an essential nitrogen donor for intracellular metabolism and maintenance of the intestines, immune cells, and muscles [14]. Numerous studies have demonstrated how glutamine metabolism influences tumor growth. For instance, studies have found that LINC01614 can directly interact with ANXA2 and p65 to promote the activation of NF-κB, leading to the upregulation of glutamine transporters SLC38A2 and SLC7A5, ultimately enhancing the metabolic uptake of glutamine in LUAD cells and promoting the LUAD progression [15]. A study on BC discovered that glutamine transporter SLC38A2 knockdown reduces glutamine metabolism and inhibits BC cell growth [16]. Therefore, future tumor diagnosis and treatment could be guided by exploring the possible mechanisms and molecular targets regulating glutamine metabolism in LUAD cells.

This study showed that the target gene S100A2 predicted by bioinformatics was highly expressed in LUAD tissues and cells, and S100A2 was significantly enriched in the glutamine metabolic pathway. S100A2 could promote the transmission of the glutamine metabolic pathway and, thus, the LUAD metastasis. In addition, TFAP2A, an upstream transcription factor of S100A2, was predicted by bioinformatics methods, and further rescue experiments confirmed that TFAP2A transcriptionally activated S100A2 expression to promote glutamine metabolism-induced metastasis of LUAD cells. However, the intrinsic molecular mechanism underlying the regulation of glutamine metabolism by the TFAP2A/S100A2 axis to promote the metastasis of LUAD cells has not been proposed yet; thus, the present study provides a new idea and theoretical basis for the theory. In conclusion, the TFAP2A/S100A2 regulatory axis has a broad development prospect in the field of LUAD metastasis research.

2 | Materials and Methods

2.1 | Sample Collection

Ten pairs of samples of LUAD and its adjacent paracancerous tissues were collected from Sichuan Mianyang 404 Hospital during the period from May 2023 to November 2023. None of the patients from whom the samples were obtained had received radiotherapy or chemotherapy, and the related research was conducted in strict accordance with the requirements of the Medical Ethics Committee of Sichuan Mianyang 404 Hospital and was approved by the committee.

2.2 | Immunohistochemistry (IHC)

Ten pairs of LUAD patients' tissues and their adjacent paracancerous tissues collected from the clinic were made into 5-μm-thick tissue sections, which were deparaffinized by formalin-fixed paraffin-embedded (FFPE) twice for 10 min each time, washed three times with PBS, and then sealed with a 5% BSA (Solarbio, China) solution at room temperature for 30 min to seal the nonspecific binding sites. After three washes with PBS, the tissue sections were incubated with primary antibody at 4°C overnight and with secondary antibody at room temperature for 30 min. The sections were washed with PBS, and the staining was visualized under a microscope using diaminobenzidine (DAB) (Lab Vision, Fremont, CA). Primary antibody rabbit anti-human S100A2 and secondary antibody goat anti-rabbit IgG H&L (HRP) were purchased from Abcam (United Kingdom).

2.3 | Bioinformatics Analysis

The LUAD mRNA expression data ("normal": 59, "tumor": 535) was obtained from The Cancer Genome Atlas (TCGA) database. The "edgeR" package was used to perform differential analysis ($|\log FC| > 1.5$, $FDR < 0.05$), and differentially expressed genes (DEGs) were screened. The target gene was identified based on the literature. Kaplan–Meier was used to analyze LUAD patient survival. The data were grouped by the median expression of the target gene. Enrichment analysis was performed by gene set enrichment analysis (GSEA) software. Upstream regulatory factors of the target gene were predicted using the hTFtarget database. The JASPAR database was used to indicate the binding site at 2000 bp upstream of S100A2 with TFAP2A.

2.4 | Cell Cultivation

293 T cells, human LUAD cell lines NCI-H1975, PC-9, and Calu-3, and the normal human lung epithelial cell line

BEAS-2B were all from BNCC (China). NCI-H1975 was cultivated in 90% Roswell Park Memorial Institute (RPMI)-1640 medium, PC-9 and BEAS-2B were cultured in 90% Dulbecco's modified Eagle's medium (DMEM)-H medium, and Calu-3 was cultured in 90% Eagle's minimal essential medium (EMEM) supplemented with 10% fetal bovine serum (FBS) and 1% penicillin/streptomycin (Beyotime, China). 293 T cells were cultivated in a medium containing 90% DMEM-H and 10% FBS with 2 mM L-glutamine. The cultivation environment was maintained at 37°C and 5% CO_2.

2.5 | Cell Transfection

si-S100A2, oe-S100A2, si-TFAP2A, and corresponding negative controls were purchased from GeneChem (China) and transfected into LUAD cells using Lipofectamine 2000 (Thermo Scientific, United States). GPNA was purchased from MCE (United States), and LUAD cells were treated with 2 mM GPNA [17].

2.6 | Quantitative Reverse Transcription Polymerase Chain Reaction (qRT-PCR)

Total RNA was extracted from cells using TRIzol reagent (Beyotime, China). RNA concentration and purity were determined using a NanoDrop ND-1000 spectrophotometer (Thermo Fisher Scientific, United States). cDNA was synthesized using the QuantiTect Reverse Transcription Kit (QIAGEN, Japan). qRT-PCR was performed on an Applied Biosystems™ 7500 real-time PCR system (Thermo Fisher Scientific, United States) by AceQ qPCR SYBR Green Master Mix (Vazyme, China). The expression of TFAP2A and S100A2 was analyzed using the $2^{-\Delta\Delta Ct}$ method. GAPDH was selected as a reference gene. The primer sequences are indicated in Table 1.

2.7 | Cell Counting Kit-8 (CCK-8) Assay

Cell viability was detected using the CCK-8 kit (Beyotime, China). Cells were seeded in 96-well plates and cultured at 37°C for 0, 24, 48, and 72 h with the addition of 10 μL of CCK-8 solution in each well. Then, cells were incubated at 37°C for 2 h, and the absorbance at 450 nm at each time point was measured using a microplate reader.

TABLE 1 | qRT-PCR primers.

Gene		Sequence
TFAP2A	Forward primer	5′-AGGTCAATCTCCCTACACGAG-3′
	Reverse primer	5′-GGAGTAAGGATCTTGCGACTGG-3′
S100A2	Forward primer	5′-TGCCAAGAGGGCGACAAGTTCA-3′
	Reverse primer	5′-AAGTCCACCTGCTGGTCACTGT-3′
GAPDH	Forward primer	5′-GGAGCGAGATCCCTCCAAAAT-3′
	Reverse primer	5′-GGCTGTTGTCATACTTCTCATGG-3′

2.8 | Immunofluorescence (IF)

The cells were placed on a glass slide and cultured, and they were washed twice with Tris-buffered saline (TBS) after discarding the cultivation medium. Then, cells were fixed with 4% paraformaldehyde fixative (prepared with TBS buffer) at 4°C for 30 min. The fixative was removed, and cells were rinsed three times with 4°C precooled TBS buffer for 5 min each and then blocked with 5% bovine serum albumin (BSA) (Solarbio, China) containing 0.1% TritonX-100 for 30 min. After washing three times with PBS, the slides were incubated with primary antibodies overnight at 4°C. Following PBS rinses, slides were incubated with fluorescent-conjugated secondary antibodies at 37°C for 2 h. DAPI (Solarbio, China) was used for nuclear DNA staining after three times washing with PBS. After cleaning, the slides were placed in antifluorescence quenching mounting fluid (Beyotime, China) and observed with a confocal microscope (Nikon, Japan). The primary antibodies are as follows: rabbit anti-human vimentin and E-cadherin. The secondary antibody is as follows: goat anti-rabbit immunoglobulin G (IgG). All antibodies in this work were purchased from Abcam (United Kingdom).

2.9 | Transwell Assay

The uncoated 8-μm-pore transwell chambers were used in the in vitro cell migration assay. In vitro cell invasion was measured using transwell chambers that had been precoated with 50 μL of Matrigel (Corning, United States). Cells in serum-free medium were placed in the upper chamber, and medium containing 10% FBS was placed in the lower chamber. Nonmigrated cells in the upper chamber were wiped off after 48 h of culture. The cells that migrated to the lower chamber were first fixed with 4% paraformaldehyde for 5 min and then stained with 0.5% crystal violet for 5 min at 25°C, and the cell migration and invasion were photographed.

2.10 | Western Blot (WB)

Cells were harvested and washed with PBS before being lysed using radioimmunoprecipitation assay (RIPA) buffer (PERFEMIKER, China) containing protease inhibitors, and the sample protein concentration was determined using a bicinchoninic acid (BCA) protein concentration assay kit (Thermo Fisher Scientific, United States). The extracted total protein was separated on a SDS-PAGE polyacrylamide gel and then transferred to a polyvinylidene fluoride (PVDF) membrane. The membrane was blocked for an hour with skim milk and incubated at 4°C with the primary antibody overnight. After being washed three times with TBS Tween-20 (TBST) buffer, the membrane was incubated for 2 h with horseradish peroxidase-labeled secondary antibodies. After TBST washing, the bands were imaged using electrochemiluminescence (ECL) immunoblotting

chemiluminescence solution and a chemiluminescence imaging system (Clinx, China), and the relative expressions of proteins were analyzed. The primary antibodies are as follows: rabbit anti-human TFAP2A, S100A2, matrix metallopeptidase 2 (MMP-2), matrix metallopeptidase 9 (MMP-9), glutaminase (GLS), glutamate dehydrogenase 1 (GLUD1), and GAPDH. The secondary antibody is as follows: goat anti-rabbit IgG H&L (HRP). The MMP-9 antibody was purchased from Cell Signal (United States), and all other antibodies were purchased from Abcam (United Kingdom).

2.11 | Glutamine Metabolite Measurement

Glutamine metabolic levels were assessed using glutamine uptake, glutamate production, and alpha-ketoglutarate (α-KG) production. The Glutamine Assay Kit (Abcam, ab197011) was used for glutamine uptake. Cells were collected in a centrifuge tube and centrifuged at 4°C for 5 min at 10000 g. Twenty microliters of the supernatant was collected and added to the corresponding well of the 96-well plate. ddH_2O was added to adjust the volume to 40 μL/well. Two microliters of the hydrolase mixture was added and thoroughly mixed. Cells were incubated in the dark for 60 min at 37°C. The microplate reader was used to measure the absorbance at 450 nm. Glutamate and α-KG production were measured using the Glutamate Assay Kit (Abcam, ab83389) and α-KG Assay Kit (Abcam, ab83431), respectively.

2.12 | GSH/GSSG and NADP/NADPH

GSH/GSSG and NADP/NADPH were determined using the GSH and GSSG assay kits (Beyotime, China) and the NADP/NADPH assay kit (Abbkine, United States), respectively.

2.13 | Dual-Luciferase Reporter Assay

pGL3-S100A2-promoter-WT and pGL3-S100A2-promoter-MUT luciferase reporter vectors (BersinBio, China) were constructed, and the two vectors were cotransfected with si-NC or si-TFAP2A into 293T cells using Lipofectamine™ 2000 (Invitrogen, United States), respectively. After 48 h of cultivation, luciferase activity was measured.

2.14 | Chromatin Immunoprecipitation (ChIP)

ChIP experiments were performed utilizing anti-IgG and anti-TFAP2A antibodies (Invitrogen, United States) and the ChIP assay kit (Merck, Germany). The precipitated DNA was tested by ChIP-qPCR. The primers are displayed in Table 2.

TABLE 2 | ChIP-qPCR primers.

Gene		Sequence
Site	Forward primer	5′-GTCTGGGGAGGACATGTGTG-3′
	Reverse primer	5′-CCAAGGCTGAAAACACCAGC-3′

2.15 | Data Analysis

Every group conducted at least three separate experiments, and the data were represented as mean ± standard deviation. Experimental data were analyzed using GraphPad Prism 8.0 for one-way ANOVA or *t*-test analysis. $p < 0.05$ was considered statistically significant.

3 | Results

3.1 | Upregulation of S100A2 Expression in LUAD

Based on the mRNA expression data of LUAD downloaded from the TCGA database, several DEGs were analyzed, and we selected S100A2 as the target gene in this study combined with the literature report [7] (Figure 1A). To study the impact of S100A2 on LUAD, we first used bioinformatics analysis to obtain the upregulated expression of S100A2 in LUAD (Figure 1B). Kaplan–Meier analysis of high S100A2 expression was positively correlated with poor prognosis in patients with LUAD (Figure 1C). IHC assay results showed that S100A2 was upregulated in LUAD tissues compared to normal tissues (Figure 1D). The qRT-PCR results indicated that the expression of S100A2 in LUAD cell lines (NCI-H1975, PC-9, and Calu-3) was much higher than that in normal human lung epithelial cells (BEAS-2B) (Figure 1E). The above research results suggested that S100A2 expression was upregulated in LUAD tissues and cells.

3.2 | S100A2 Enhances LUAD Metastasis

To verify the influence of S100A2 on LUAD metastasis, S100A2 knockdown and overexpression cell groups were constructed based on PC-9 and Calu-3 cells. Through qRT-PCR, it was found that si-S100A2 greatly inhibited the S100A2 expression in PC-9 cells, and oe-S100A2 notably promoted the S100A2 expression in Calu-3 cells (Figure 2A). CCK-8 experiment results demonstrated that si-S100A2 greatly inhibited cell viability, while oe-S100A2 did the opposite (Figure 2B). Transwell assay results indicated that PC-9 cell migration and invasion capabilities were markedly decreased in the si-S100A2 group, while Calu-3 cell capacity for migration and invasion in the oe-S100A2 group was noticeably enhanced (Figure 2C). Next, the expression of EMT-related proteins vimentin and E-cadherin was determined by IF. The results suggested that the expression of vimentin was reduced and the expression of E-cadherin was increased in PC-9 cells of the si-S100A2 group, while the reverse trend was observed in the oe-S100A2 group (Figure 2D). MMP-2 and MMP-9 are members of the matrix metalloproteinase (MMP) family, collectively known as gelatinases. In previous studies, gelatinases and other MMPs were commonly associated with invasion, metastasis, and angiogenesis in solid tumors [18]. Therefore, MMP-2 and MMP-9 are called metastasis-associated proteins. Finally, the expression of

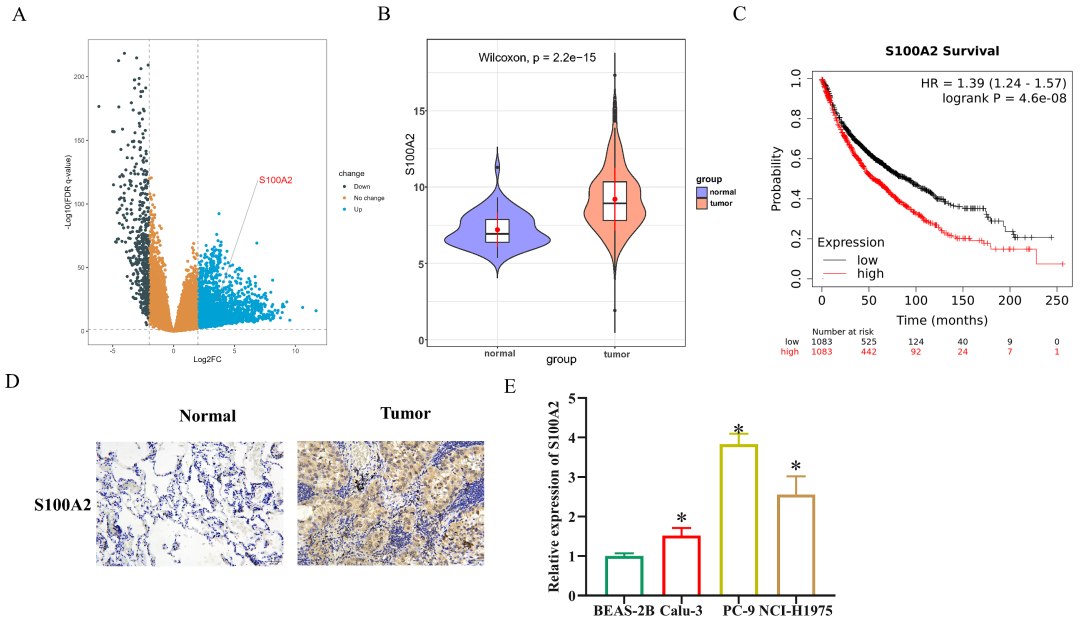

FIGURE 1 | S100A2 expression in LUAD. (A) Volcano plot based on mRNA differential analysis in the TCGA-LUAD dataset. (B) Bioinformatics analysis of S100A2 expression in LUAD tissues. (C) Kaplan–Meier analysis of S100A2 expression in relation to survival in LUAD patients. (D) S100A2 expression in LUAD tissues. (E) S100A2 expression in LUAD cells. * represents $p < 0.05$.

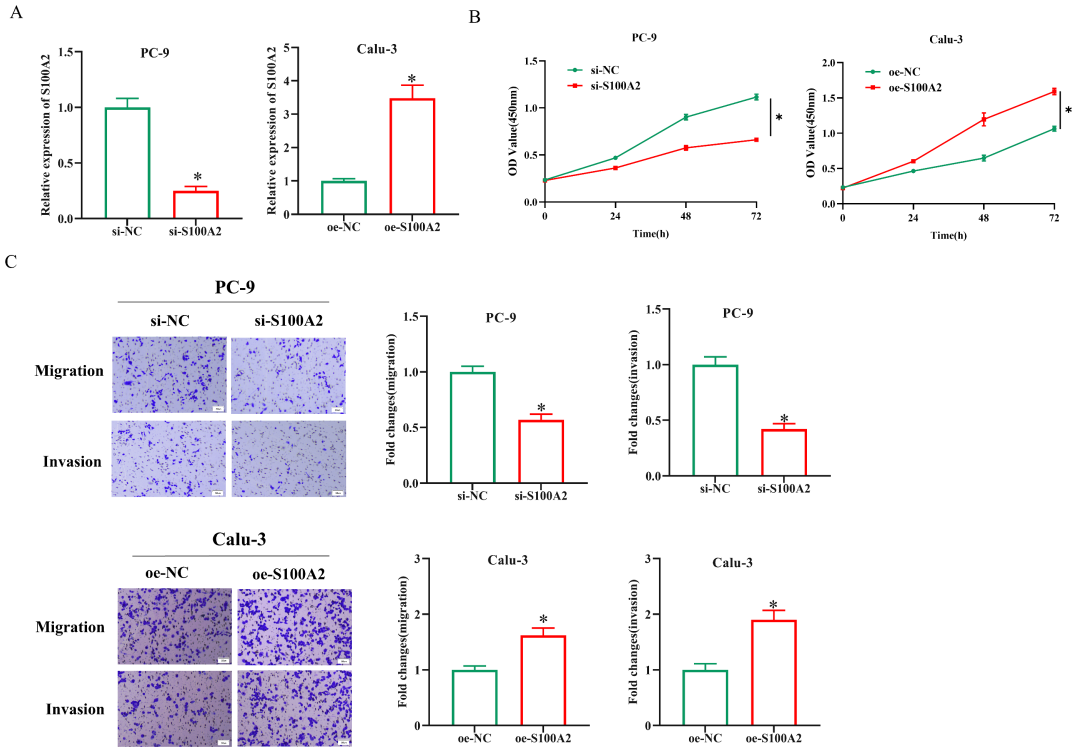

FIGURE 2 | S100A2 promotes LUAD metastasis. (A) S100A2 expression detection. (B) Cell viability determination. (C) Cell migration and invasion ability determination. The scale bar was 50 μm. (D) EMT-related protein expression detection. The scale bar was 50 μm. (E) Metastasis-related protein expression detection. * represents $p < 0.05$.

metastasis-related proteins (MMP-2 and MMP-9) was detected by WB. S100A2 knockdown inhibited the expression of MMP-2 and MMP-9 in PC-9 cells, while S100A2 overexpression stimulated MMP-2 and MMP-9 expression in Calu-3 cells (Figure 2E). These results proved that S100A2 could promote LUAD metastasis at the cellular level.

3.3 | S100A2-Mediated Glutamine Metabolism Affects LUAD Metastasis

To investigate the regulatory effect of S100A2 on LUAD metastasis, S100A2 was found to be enriched in the glutamine metabolic pathway through bioinformatics analysis (Figure 3A), and

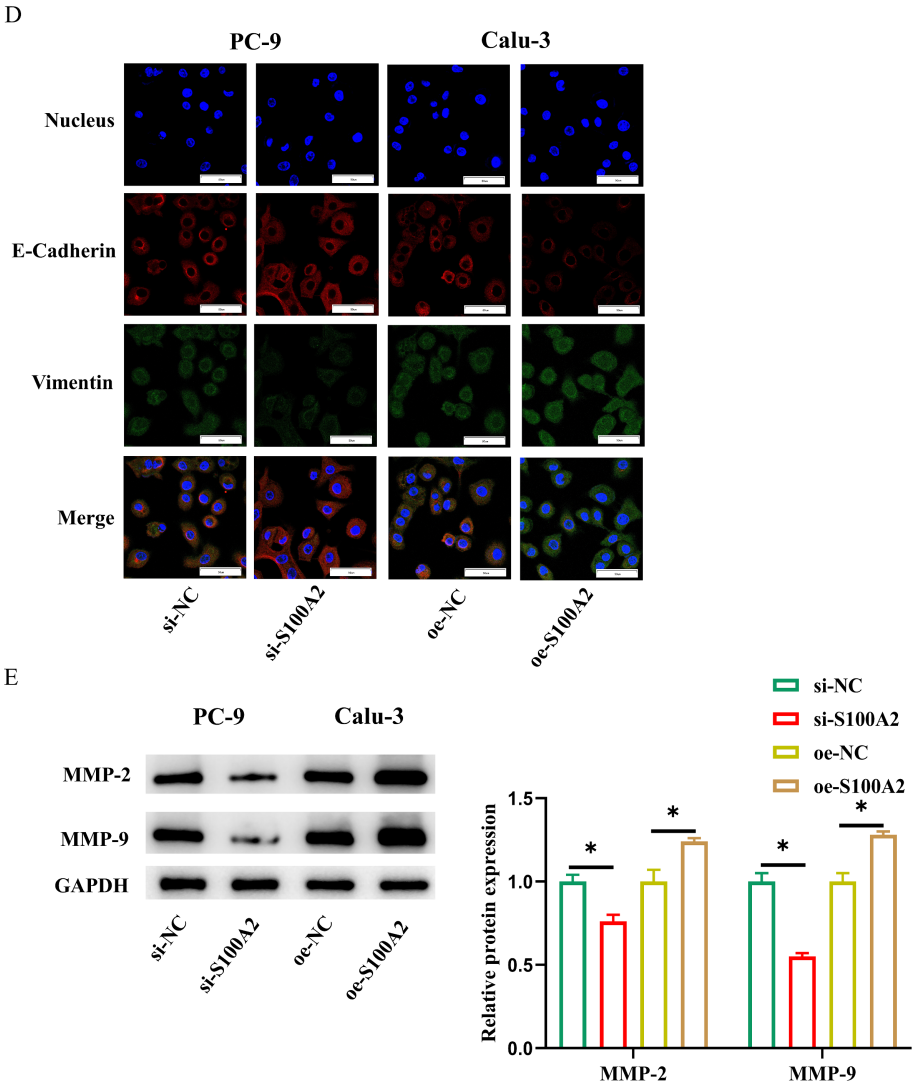

FIGURE 2 | Continued.

Pearson's correlation analysis demonstrated that S100A2 was positively correlated with the key gene SLC38A5 in glutamine metabolism (Figure 3B). Subsequently, S100A2 knockdown and overexpression cell lines were constructed. GLS and GLUD1 are glutamine metabolism-associated proteins, and it has been demonstrated that IGF2BP3 stabilizes the gene expression of GLS and GLUD1 through m6A modification and promotes glutamate and glutamine metabolism in human cervical cancer cells [19]. The expression of glutamine metabolism-related proteins GLS, GLUD1, and SLC38A5 was determined by WB. The results indicated that the expression of SLC38A5, glutamine metabolism-related proteins GLS, and GLUD1 in PC-9 cells of the si-S100A2 group was greatly reduced. In contrast, the expression of SLC38A5, GLS, and GLUD1 in Calu-3 cells in the oe-S100A2 group was noticeably increased (Figure 3C). The metabolic level of glutamine was then evaluated, and it was found that glutamine consumption, glutamate, and α-KG production were reduced in PC-9 cells in the si-S100A2 group, while the opposite trend was observed in the oe-S100A2 group (Figure 3D–F). The NADP/NADPH and GSH/GSSG ratios were further measured, and it was found that the NADP/NADPH ratio increased and the GSH/GSSG ratio decreased in PC-9 cells of the si-S100A2 group, while the opposite trend was observed in the oe-S100A2 group (Figure 3G,H). Groups were reestablished based on Calu-3 cells: oe-NC + DMSO, oe-S100A2 + DMSO, and oe-S100A2 + GPNA (selective inhibitor of glutamine transporter alanine–serine–cysteine transporter 2 [ASCT2]). The CCK-8 detection results suggested that Calu-3 cell viability was greatly increased by overexpressing S100A2, and when GPNA was added, cell viability returned to the control level (Figure 3I). According to transwell results, overexpression of S100A2 enhanced Calu-3 cell capacities for migration and invasion, while the addition of GPNA reduced the effect of overexpression of S100A2 on these capacities (Figure 3J,K). Vimentin expression was enhanced, and E-cadherin expression was suppressed by upregulation of S100A2, according to IF results. After adding GPNA, the expressions of vimentin and E-cadherin returned to the control level (Figure 3L). Finally, the expression of SLC38A5 and metastasis-related proteins (MMP-2 and MMP-9) was detected by WB. SLC38A5, MMP-2, and MMP-9 expressions were found to be substantially elevated by upregulating S100A2, whereas the addition of GPNA inhibited the promoting effect of S100A2 overexpression on MMP-2 and MMP-9 protein expression without impact on SLC38A5 protein expression (Figure 3M). These results indicated that S100A2 mediated glutamine metabolism to enhance the LUAD progression.

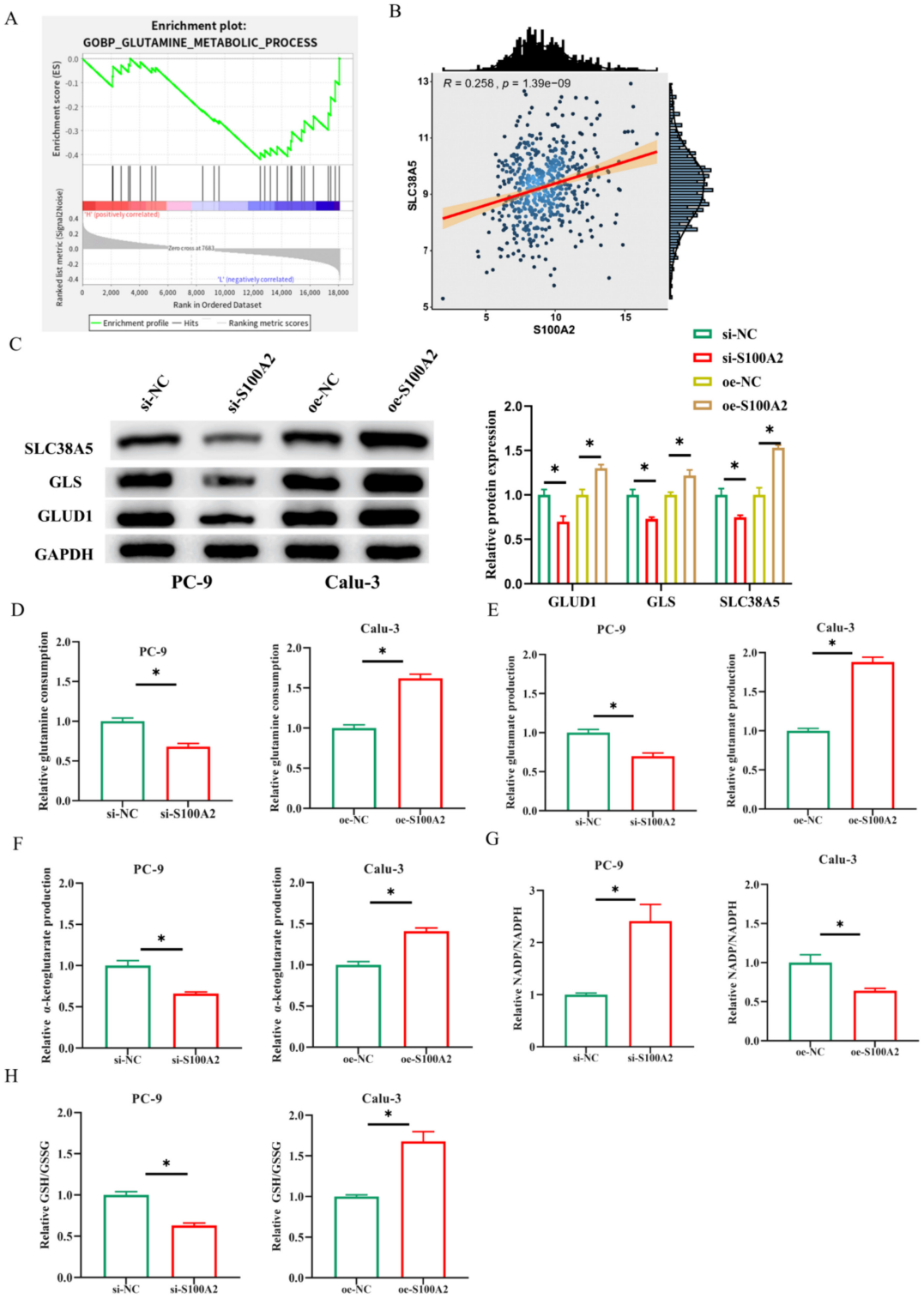

FIGURE 3 | S100A2-mediated glutamine metabolism affects LUAD metastasis. (A) Enrichment pathway analysis. (B) Correlation analysis of S100A2 and glutamine metabolic marker genes. (C) SLC38A5, GLS, and GLUD1 expression detection. (D–F) Determination of glutamine consumption, glutamate content, and α-KG content. (G, H) NADP/NADPH and GSH/GSSG ratios. (I) Cell viability detection. (J, K) Cell migration and invasion determination. The scale bar was 50 μm. (L) Vimentin and E-cadherin expression detection. The scale bar was 50 μm. (M) MMP-2 and MMP-9 expression detection. * represents $p < 0.05$.

3.4 | The Regulatory Relationship Between TFAP2A and S100A2 in LUAD

To study the potential mechanism of S100A2 affecting LUAD, bioinformatics analysis and correlation analysis were performed. The expression of the upstream transcription factor TFAP2A was positively correlated with S100A2 (Figure 4A,B). There was a potential binding site between the TFAP2A and S100A2 transcripts at 2000 bp upstream in the JASPAR database (Figure 4C). Bioinformatics analysis revealed that LUAD

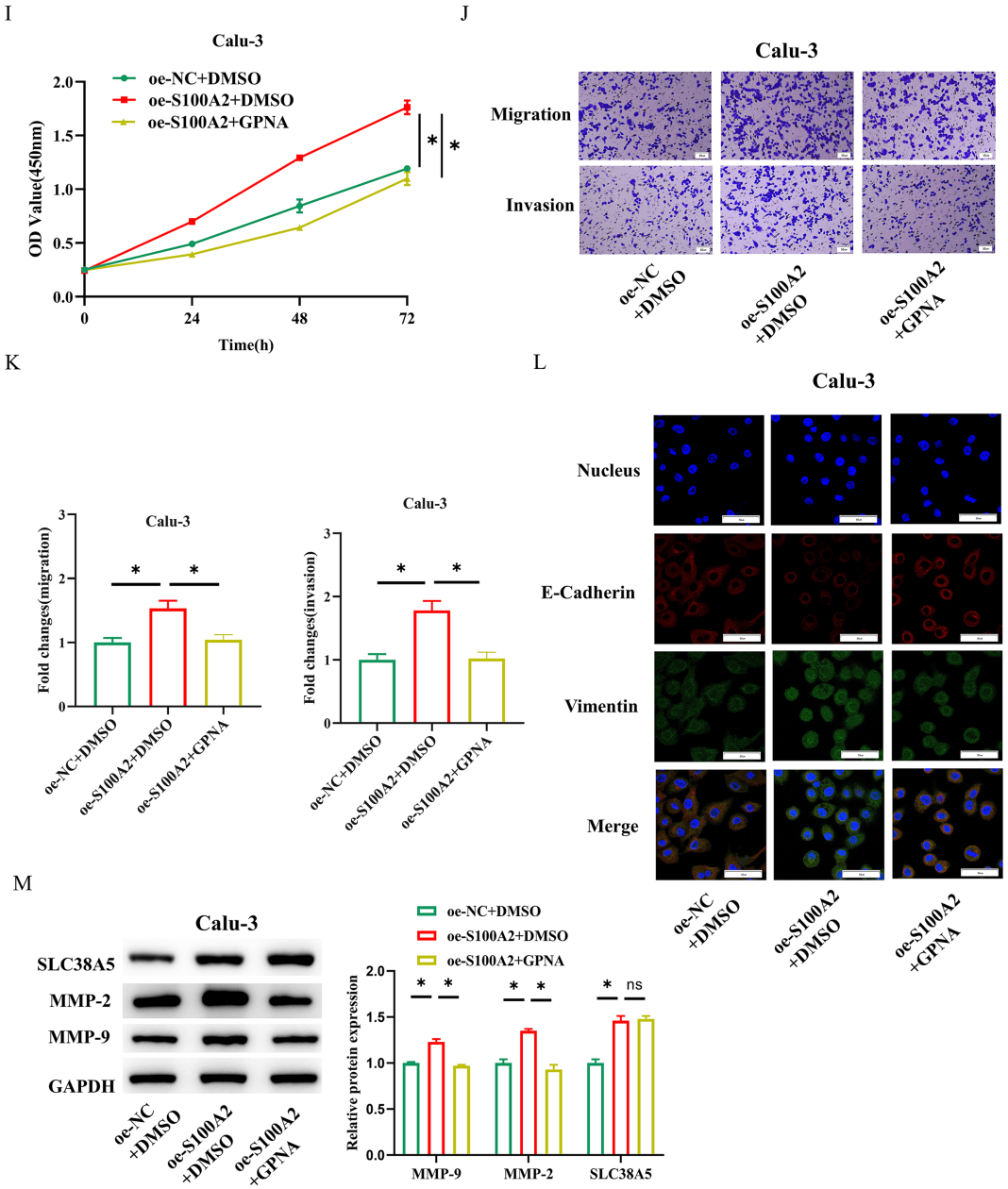

FIGURE 3 | Continued.

tissues had high levels of TFAP2A expression (Figure 4D), and TFAP2A was also found to be highly expressed in LUAD cells by qRT-PCR detection (Figure 4E). Next, dual luciferase assay results suggested that TFAP2A silencing could reduce the luciferase activity of wild-type S100A2 but had no discernible impact on mutant S100A2 (Figure 4F). ChIP results demonstrated that anti-TFAP2A could greatly increase S100A2 enrichment (Figure 4G). According to the results above, TFAP2A facilitated S100A2 expression.

3.5 | TFAP2A Enhances S100A2 Expression to Induce LUAD Metastasis Through Glutamine Metabolism

Based on PC-9 cells, we constructed knockdown TFAP2A cells and TFAP2A knockdown combined with S100A2 overexpression cells to further investigate the influence of TFAP2A on LUAD metastasis by enhancing S100A2 expression. First, qRT-PCR was used to detect the S100A2 expression level in each group. The results indicated that si-TFAP2A greatly inhibited S100A2 expression in PC-9 cells. Knockdown of TFAP2A and overexpression of S100A2 in PC-9 cells restored the expression of S100A2 to the control level (Figure 5A). CCK-8 results suggested that si-TFAP2A inhibited PC-9 cell viability, while oe-S100A2 could reverse the inhibitory effect of si-TFAP2A on cell viability (Figure 5B). According to transwell assay results, PC-9 cell invasion and migration were dramatically suppressed by si-TFAP2A. Knockdown of TFAP2A and overexpression of S100A2 restored the migration and invasion abilities of cells to the control level (Figure 5C). IF detection results indicated that si-TFAP2A greatly decreased vimentin expression and dramatically increased E-cadherin expression in PC-9 cells, but simultaneously overexpressing S100A2 restored the expression

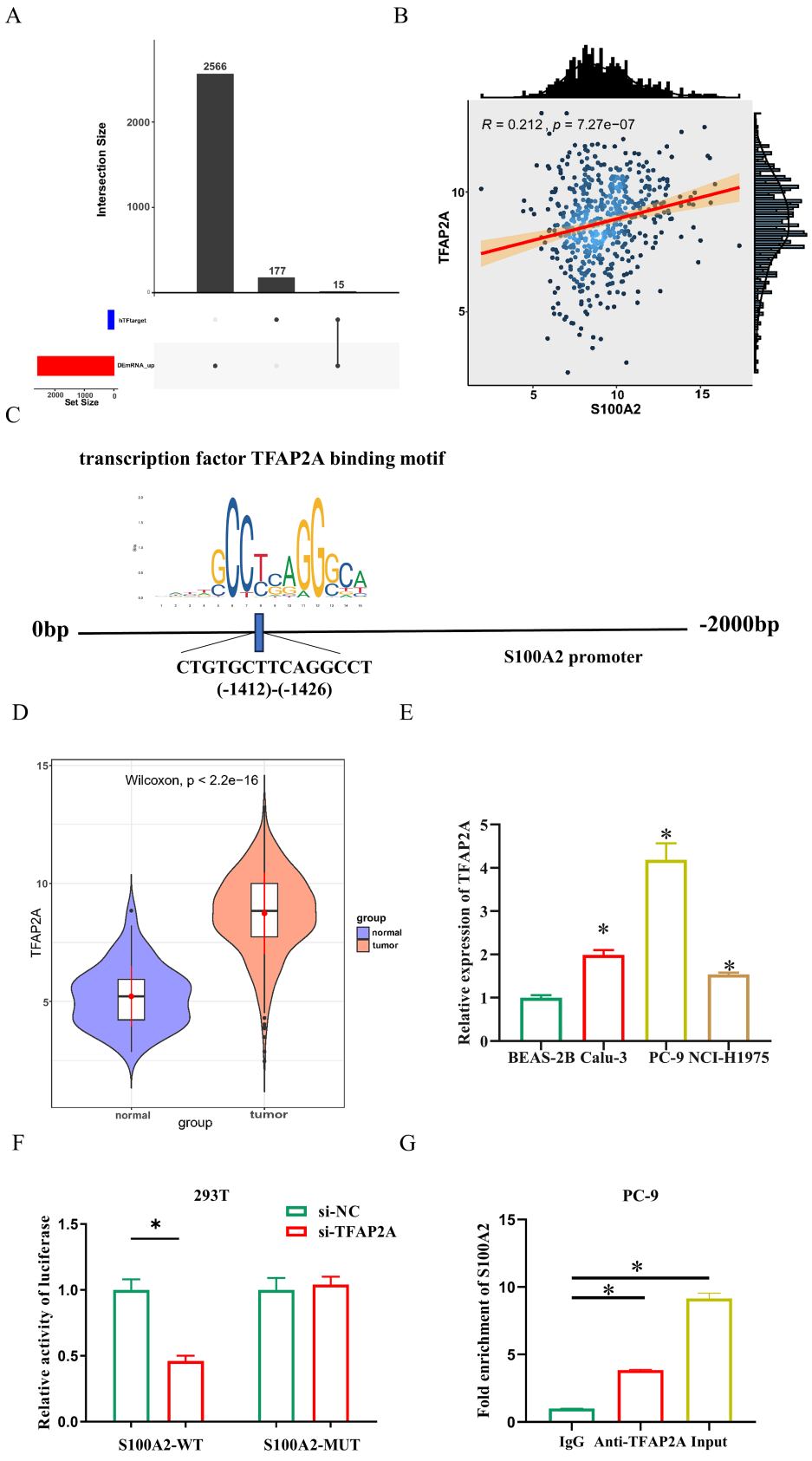

FIGURE 4 | TFAP2A affects the S100A2 expression in LUAD. (A) Upset plot of S100A2 predicted upstream target genes and differentially expressed genes. (B) Expression correlation between TFAP2A and S100A2. (C) TFAP2A and S100A2 target binding sites. (D) TFAP2A expression in LUAD tissue. (E) TFAP2A expression in LUAD cells. (F, G) Verification of the TFAP2A and S100A2 binding relationship. * represents $p < 0.05$.

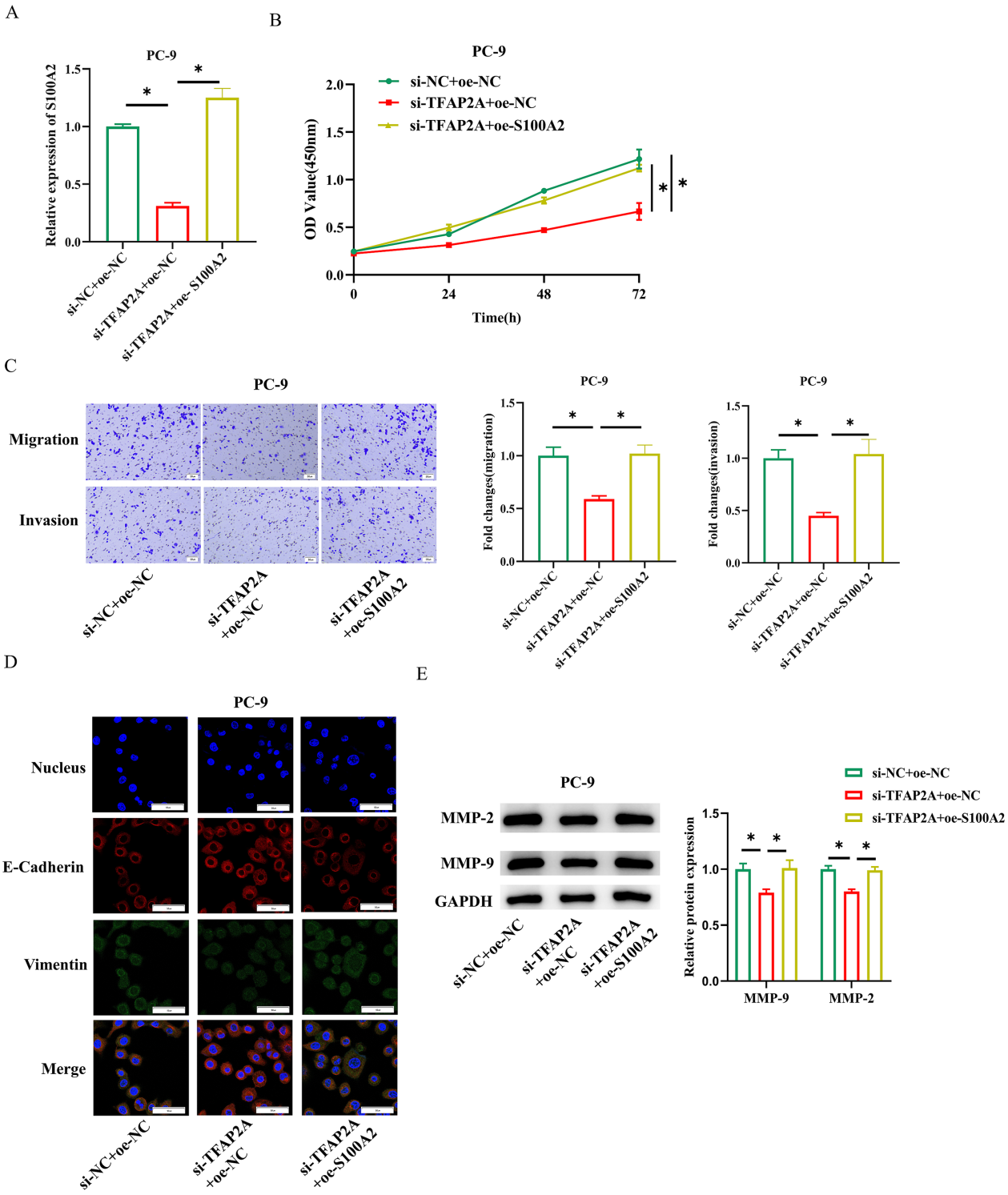

FIGURE 5 | TFAP2A increases S100A2-mediated glutamine metabolism to induce LUAD metastasis. (A) S100A2 expression in LUAD. (B) Cell viability determination. (C) Cell migration and invasion determination. The scale bar was 50 μm. (D) Vimentin and E-cadherin expression detection. The scale bar was 50 μm. (E) MMP-2 and MMP-9 expression detection. (F–H) Glutamine consumption, glutamate content, and α-KG content determination. (I) NADP/NADPH and GSH/GSSG ratio determination. (J) GLS and GLUD1 expression detection. * represents $p < 0.05$.

of vimentin and E-cadherin to the control level (Figure 5D). According to WB detection, the expression of the metastasis-related proteins MMP-2 and MMP-9 was markedly decreased by si-TFAP2A in PC-9 cells, but simultaneously overexpressing S100A2 could reverse this inhibitory effect (Figure 5E). Measurement of glutamine metabolism levels in LUAD found that after knocking down TFAP2A, glutamine was consumed, glutamate and α-KG were reduced, but simultaneously upregulating S100A2 could reverse this effect (Figure 5F–H). NADP/NADPH and GSH/GSSG were evaluated, and it was found that

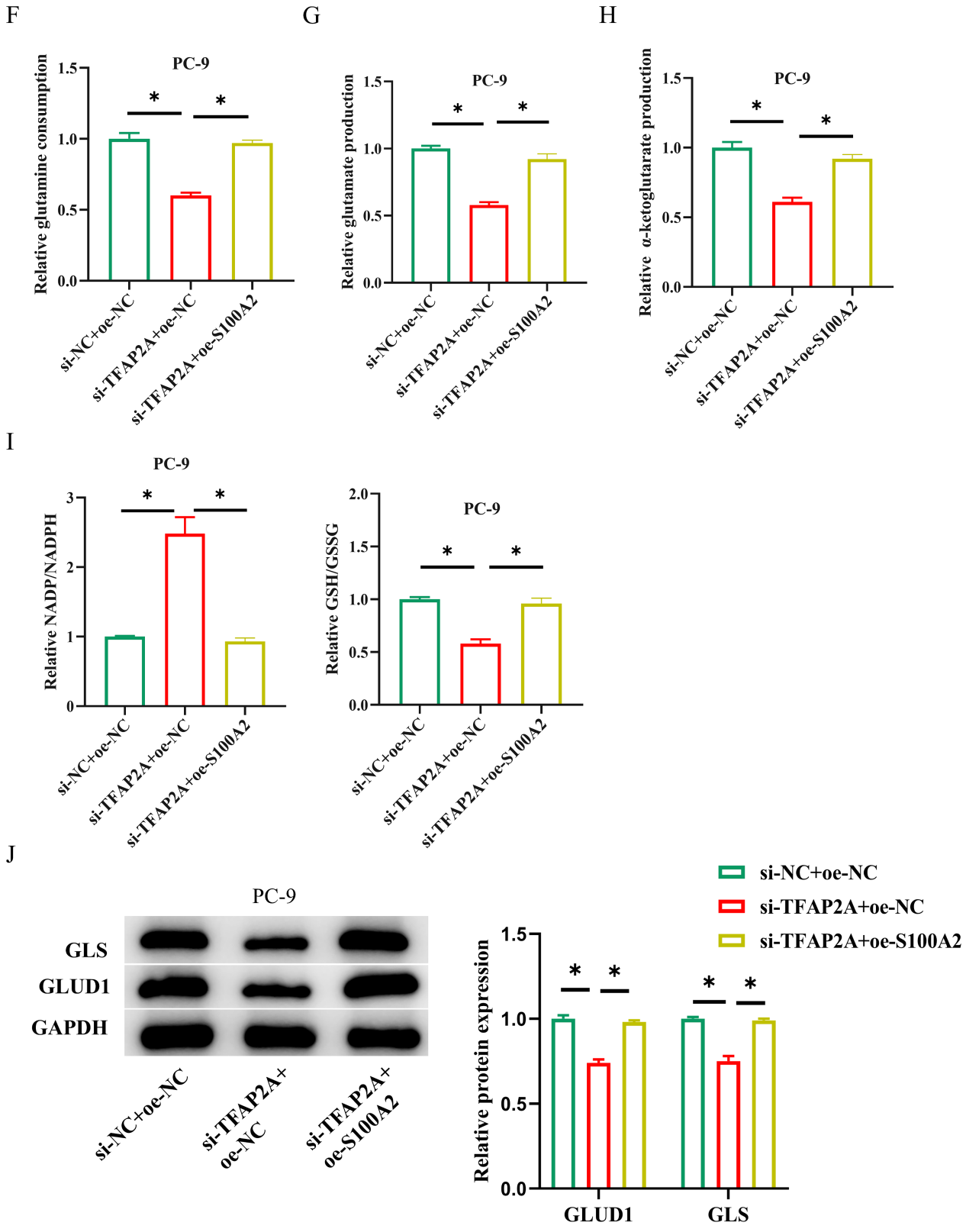

FIGURE 5 | Continued.

silencing TFAP2A tended to favor NADP and GSSG, while the two ratios returned to the control level with concurrent transfection of oe-S100A2 (Figure 5I). Finally, the expression of glutamine metabolism-related proteins GLS and GLUD1 was detected by WB. It was found that si-TFAP2A greatly reduced the expression of GLS and GLUD1 in PC-9 cells, but simultaneously overexpressing S100A2 restored the expression of GLS and GLUD1 to the control group level (Figure 5J). In summary, TFAP2A could upregulate S100A2 to mediate glutamine metabolism to induce LUAD metastasis.

4 | Discussion

S100A2 dysregulation is linked to the etiology of many cancers. Studies have evidenced that S100A2 is abnormally expressed in various cancer tissues and cells. Li et al. found that S100A2 expression is markedly upregulated in CRC [20]. In an investigation on EC, it was discovered that EC has noticeably higher levels of S100A2 expression [11]. Consistent with the previous conclusion, this investigation demonstrated the substantial upregulation of S100A2 in LUAD tissues and cells. Tumor invasion, metastasis, and proliferation are typically associated with abnormal expression of S100A2. Studies have validated that S100A2 expression is enhanced by DNA methylation-related hypoxia/HIF-1α signaling in hepatocellular carcinoma (HCC). Under hypoxic conditions, HCC cell proliferation and invasion are markedly suppressed by S100A2 knockdown [10]. A study on papillary thyroid cancer (PTC) discovered that by upregulating S100A2 expression, miR-181a can encourage PTC cell proliferation, invasion, and migration [21]. Similarly, our findings revealed that S100A2 overexpression strongly encouraged LUAD cell migration and invasion. Based on these findings, it is possible to use S100A2 as a therapeutic target and diagnostic marker for LUAD, as it was found to have a prometastatic role in tumor mechanisms.

Glutamine is considered a substrate source for the tricarboxylic acid cycle and is essential for the survival and adaptation of cancer cells. GLS is a key enzyme in glutamine metabolism. Studies have found that knocking down GLS reduces the decomposition of glutamate in triple-negative BC cells, inhibits glutamine metabolism, and reduces the growth and metastasis of tumor cells [22]. Angiopoietin-like protein (ANGPTL) 4 can upregulate the expression of GLS and carnitine palmitoyltransferase I (CPT1), enhance glutamine metabolism, and accelerate the development of non–small cell lung cancer [23]. Consistent with the previous studies, the results of this study proved that knocking down S100A2 resulted in decreased glutamine consumption and decreased expression of the proteins related to glutamine metabolism, GLS, and GLUD1. ASCT2 is a key glutamine transporter. Studies have verified that MLN4924 regulates glutamine metabolism through ASCT2 to promote BC progression [24]. In this research, S100A2 overexpression markedly increased LUAD glutamine metabolism, while this promotion effect was decreased by the addition of GPNA. In summary, tumor metabolic reprogramming is essential to tumor progression. Therefore, studying the molecular mechanism by which glutamine metabolism affects tumor progression is of great significance for the future treatment of glutamine-dependent LUAD patients. Our data also further supported that targeting the glutamine metabolic pathway may be a potential therapeutic strategy to inhibit LUAD metastasis.

In this work, TFAP2A expression was upregulated in LUAD, and TFAP2A binding with the S100A2 promoter region stimulated the S100A2 transcription. Transcription factor TFAP2A is an important cell-growing regulatory factor and is highly expressed in pancreatic cancer [25], ovarian cancer [26], basal-squamous bladder cancer [27], and other tumors. It is reported that TFAP2A is highly expressed in cervical cancer, and silencing TFAP2A inhibits the proliferation and migration of cervical cancer cells [28]. Another research pointed out that TFAP2A induces ITPKA overexpression and interacts with DBN1 to facilitate EMT, which in turn enhances LUAD migration and proliferation [29]. According to our results, TFAP2A knockdown changed the expression of EMT-related proteins and inhibited the metastasis of LUAD cells, but simultaneously, overexpression of S100A2 reversed the effect of TFAP2 knockdown. These results suggested that TFAP2A regulated LUAD metastasis by regulating S100A2 transcription. These findings contributed to the understanding of the indirect involvement of S100A2 in the progression of LUAD.

In summary, this study explored TFAP2A as a transcription factor that activated the S100A2 transcription and mediated glutamine metabolism to affect the LUAD progression. The results indicated that TFAP2A activated S100A2 to mediate glutamine metabolism and induce LUAD metastasis. This study suggested that targeting the TFAP2A/S100A2 axis may be a promising strategy for the LUAD treatment. However, this work still has shortcomings. The promoting role of the TFAP2A/S100A2 axis in LUAD metastasis and the potential interaction of S100A5 with other small molecules, such as SLC38A5, have not been further verified through animal experiments. In the future, we will delve deeper into the veracity of this theory through animal models. In conclusion, our study elucidated the impact of the TFAP2A/S100A2 axis on LUAD metastasis and provided insights for developing new treatments for LUAD.

Author Contributions

Conception and design: Tao Zeng. Administrative support: Wangsheng Ren. Provision of study materials or patients: Tao Zeng and Hang Zeng. Collection and assembly of data: Dachun Wang. Data analysis and interpretation: Xianyu Wu and Guo Xu. Manuscript writing: all authors. Final approval of manuscript: all authors.

Ethics Statement

The related research was approved by the Medical Ethics Committee of Sichuan Mianyang 404 Hospital, approval number: 2024-015.

Conflicts of Interest

The authors declare no conflicts of interest.

Data Availability Statement

The data that support the findings of this study are available from the corresponding author upon reasonable request.

References

1. R. L. Siegel, K. D. Miller, N. S. Wagle, and A. Jemal, "Cancer Statistics, 2023," *CA: A Cancer Journal for Clinicians* 73, no. 1 (2023): 17–48.

2. D. Kerdidani, P. Chouvardas, A. R. Arjo, et al., "Wnt1 Silences Chemokine Genes in Dendritic Cells and Induces Adaptive Immune Resistance in Lung Adenocarcinoma," *Nature Communications* 10, no. 1 (2019): 1405.

3. C. Zhang, J. Zhang, F. P. Xu, et al., "Genomic Landscape and Immune Microenvironment Features of Preinvasive and Early Invasive Lung Adenocarcinoma," *Journal of Thoracic Oncology* 14, no. 11 (2019): 1912–1923.

4. V. Jurisic, V. Vukovic, J. Obradovic, L. F. Gulyaeva, N. E. Kushlinskii, and N. Djordjevic, "EGFR Polymorphism and Survival of NSCLC

Patients Treated With TKIs: A Systematic Review and Meta-Analysis," *Journal of Oncology* 2020 (2020): 1–14.

5. L. L. Gonzalez, K. Garrie, and M. D. Turner, "Role of S100 Proteins in Health and Disease," *Biochimica et Biophysica Acta, Molecular Cell Research* 1867, no. 6 (2020): 118677.

6. M. A. Raffat, N. I. Hadi, M. Hosein, S. Mirza, S. Ikram, and Z. Akram, "S100 Proteins in Oral Squamous Cell Carcinoma," *Clinica Chimica Acta* 480 (2018): 143–149.

7. T. Wang, G. Du, and D. Wang, "The S100 Protein Family in Lung Cancer," *Clinica Chimica Acta* 520 (2021): 67–70.

8. G. Huang, J. Zhang, G. Qing, et al., "S100A2 Silencing Relieves Epithelial-Mesenchymal Transition in Pulmonary Fibrosis by Inhibiting the Wnt/Beta-Catenin Signaling Pathway," *DNA and Cell Biology* 40, no. 1 (2021): 18–25.

9. H. Sugino and Y. Sawada, "Influence of S100A2 in Human Diseases," *Diagnostics (Basel)* 12, no. 7 (2022): 1756.

10. J. Yan, Y. J. Huang, Q. Y. Huang, P. X. Liu, and C. S. Wang, "Transcriptional Activation of S100A2 Expression by HIF-1Alpha via Binding to the Hypomethylated Hypoxia Response Elements in HCC Cells," *Molecular Carcinogenesis* 61, no. 5 (2022): 494–507.

11. Q. Zhang, T. Xia, C. Qi, J. Du, and C. Ye, "High Expression of S100A2 Predicts Poor Prognosis in Patients With Endometrial Carcinoma," *BMC Cancer* 22, no. 1 (2022): 77.

12. F. Han, L. Zhang, S. Liao, et al., "The Interaction Between S100A2 and KPNA2 Mediates NFYA Nuclear Import and Is a Novel Therapeutic Target for Colorectal Cancer Metastasis," *Oncogene* 41, no. 5 (2022): 657–670.

13. H. Wang, X. Hu, F. Yang, and H. Xiao, "miR-325-3p Promotes the Proliferation, Invasion, and EMT of Breast Cancer Cells by Directly Targeting S100A2," *Oncology Research* 28, no. 7 (2021): 731–744.

14. J. Zhang, N. N. Pavlova, and C. B. Thompson, "Cancer Cell Metabolism: The Essential Role of the Nonessential Amino Acid, Glutamine," *EMBO Journal* 36, no. 10 (2017): 1302–1315.

15. T. Liu, C. Han, P. Fang, et al., "Cancer-Associated Fibroblast-Specific lncRNA LINC01614 Enhances Glutamine Uptake in Lung Adenocarcinoma," *Journal of Hematology & Oncology* 15, no. 1 (2022): 141.

16. M. Morotti, C. E. Zois, R. El-Ansari, et al., "Increased Expression of Glutamine Transporter SNAT2/SLC38A2 Promotes Glutamine Dependence and Oxidative Stress Resistance, and Is Associated With Worse Prognosis in Triple-Negative Breast Cancer," *British Journal of Cancer* 124, no. 2 (2021): 494–505.

17. W. Wang, H. Pan, F. Ren, H. Chen, and P. Ren, "Targeting ASCT2-Mediated Glutamine Metabolism Inhibits Proliferation and Promotes Apoptosis of Pancreatic Cancer Cells," *Bioscience Reports* 42 (2022): 42 (3).

18. S. Das, S. A. Amin, and T. Jha, "Inhibitors of Gelatinases (MMP-2 and MMP-9) for the Management of Hematological Malignancies," *European Journal of Medicinal Chemistry* 223 (2021): 113623.

19. T. Zhou, Z. Xiao, J. Lu, L. Zhang, L. Bo, and J. Wang, "IGF2BP3-Mediated Regulation of GLS and GLUD1 Gene Expression Promotes Treg-Induced Immune Escape in Human Cervical Cancer," *American Journal of Cancer Research* 13, no. 11 (2023): 5289–5305.

20. C. Li, Q. Chen, Y. Zhou, et al., "S100A2 Promotes Glycolysis and Proliferation via GLUT1 Regulation in Colorectal Cancer," *FASEB Journal* 34, no. 10 (2020): 13333–13344.

21. Y. Wang, H. Ye, Y. Yang, J. Li, A. Cen, and L. Zhao, "microRNA-181a Promotes the Oncogene S100A2 and Enhances Papillary Thyroid Carcinoma Growth by Mediating the Expression of Histone Demethylase KDM5C," *Journal of Endocrinological Investigation* 45, no. 1 (2022): 17–28.

22. D. N. Edwards, V. M. Ngwa, A. L. Raybuck, et al., "Selective Glutamine Metabolism Inhibition in Tumor Cells Improves Antitumor T Lymphocyte Activity in Triple-Negative Breast Cancer," *Journal of Clinical Investigation* 131 (2021): 131 (4).

23. S. Xiao, W. Nai-Dong, Y. Jin-Xiang, et al., "ANGPTL4 Regulate Glutamine Metabolism and Fatty Acid Oxidation in Nonsmall Cell Lung Cancer Cells," *Journal of Cellular and Molecular Medicine* 26, no. 7 (2022): 1876–1885.

24. Q. Zhou, W. Lin, C. Wang, et al., "Neddylation Inhibition Induces Glutamine Uptake and Metabolism by Targeting CRL3(SPOP) E3 Ligase in Cancer Cells," *Nature Communications* 13, no. 1 (2022): 3034.

25. J. Wu, "Pancreatic Cancer-Derived Exosomes Promote the Proliferation, Invasion, and Metastasis of Pancreatic Cancer by the miR-3960/TFAP2A Axis," *Journal of Oncology* 2022 (2022): 3590326.

26. H. Xu, L. Wang, and X. Jiang, "Silencing of lncRNA DLEU1 Inhibits Tumorigenesis of Ovarian Cancer via Regulating miR-429/TFAP2A Axis," *Molecular and Cellular Biochemistry* 476, no. 2 (2021): 1051–1061.

27. H. Yamashita, Y. I. Kawasawa, L. Shuman, et al., "Repression of Transcription Factor AP-2 Alpha by PPARgamma Reveals a Novel Transcriptional Circuit in Basal-Squamous Bladder Cancer," *Oncogene* 8, no. 12 (2019): 69.

28. J. Yang, Y. Gao, S. Yao, S. Wan, and H. Cai, "TFAP2A Promotes Cervical Cancer via a Positive Feedback Pathway With PD-L1," *Oncology Reports* 49 (2023): 1–14.

29. Z. Guoren, F. Zhaohui, Z. Wei, et al., "TFAP2A Induced ITPKA Serves as an Oncogene and Interacts With DBN1 in Lung Adenocarcinoma," *International Journal of Biological Sciences* 16, no. 3 (2020): 504–514.